Energy Capture Optimization for an Adaptive Wave Energy Converter

Barradas Berglind, Jose de Jesus; Meijer, Harmen; van Rooij, Marijn; Clemente Pinol, Silvia; Galvan Garcia, Bruno; Prins, Wouter; Vakis, Antonis I.; Jayawardhana, Bayu

Published in:
Proceedings of the 2nd International Conference on Renewable Energies Offshore - RENEW 2016

Publication date:
2016

Energy capture optimization for an adaptive wave energy converter

J.J. Barradas-Berglind, H. Meijer, M. van Rooij, S. Clemente-Piñol, B. Galván-García, W.A. Prins, A.I. Vakis & B. Jayawardhana
Engineering and Technology Institute Groningen, Faculty of Mathematics and Natural Sciences University of Groningen, Groningen, The Netherlands.

ABSTRACT: Wave energy has great potential as a renewable energy source, and can therefore contribute significantly to the proportion of renewable energy in the global energy mix. This is especially important since energy mixes with high renewable penetration have become a worldwide priority. One solution to facilitate such goals is to harvest the latent untapped energy of the ocean waves and convert it into electrical energy. A device performing such a task is known as a wave energy converter (WEC). In the present work, we focus on a specific type of WEC, which has the advantages of both significant energy storage capabilities, and adaptability to extract energy from the whole spectrum of ocean waves. This WEC consists of an array of point absorber devices, comprising adaptable piston-type hydraulic pumps powered by interconnected floaters, whose target is to extract optimally the energy from waves of varying heights and periods. Two different cases are considered in this paper; namely, the analysis of the energy extraction in a simplified floater blanket, and a model predictive control strategy to maximize the extracted energy of the WEC.

1 INTRODUCTION

Increased renewable energy penetration in countries' energy mix has become a worldwide priority, evidenced, for example, by the Kyoto Protocol, and the more recent COP 21 held in Paris. Wave energy is one renewable energy source that shows great promise and is a viable alternative to facilitate the aforementioned energy mix goals. This can be achieved by converting the latent untapped energy of the ocean waves into electrical energy through a device known as a wave energy converter (WEC). There are diverse operating principles of WECs such as oscillating water columns, connected structures, overtopping devices, and point absorbers (Drew, Plummer, & Sahinkaya 2009, Koca, Kortenhaus, Oumeraci, Zanuttigh, Angelelli, Cantu, Suffredini, & Franceschi 2013, Ringwood, Bacelli, & Fusco 2014). A comprehensive exposition of different types of WECs can be found in (Ringwood, Bacelli, & Fusco 2014) and the references therein from a control engineering perspective, and in (SI-Ocean 2012) from a broader perspective.

The focus of this paper is on a specific WEC with a novel power take-off (PTO) system; this PTO is comprised of interconnected floaters attached to adaptable piston-type hydraulic pumps, whose target is to extract the energy from waves of varying heights and periods. Its adaptability to different types of waves is one of the main strengths of this WEC, which requires several buoys in a column to extract most of the wave energy in a sequential manner. The WEC is part of the Ocean Grazer, which is a novel ocean energy collection and storage device, designed to extract and store multiple forms of ocean energy (Vakis, Meijer, & Prins 2014, van Rooij, Meijer, Prins, & Vakis 2015, Vakis & Anagnostopoulos 2016).

The contributions of this paper are twofold with regard to the technological development of the Ocean Grazer: (I) the analysis of the wave energy extraction through a simple floater blanket system; and (II) the control design of the adaptable piston pumps for optimal energy extraction for arbitrary wave profiles. The first case focuses on the energy extraction of an array of floaters connected to pumping systems. In this analysis, we consider the dynamical interactions between buoys, pumps and storage elements. This also includes the radiating waves between buoys. In the second case, we propose a model predictive control (MPC) strategy in order to maximize the energy capture from the waves. The proposed solution relies on mathematical optimization (Bertsekas 1999, Papalambros & Wilde 2000), which aims at maximizing the extracted energy from the waves. In (Li, Weiss, Mueller, Townley, & Belmont 2012) the applicability of MPC for optimizing a single non-adaptable WEC is discussed —by non-adaptability we mean that the WEC operation is restricted to a certain wave height. In (Feng & Kerrigan 2013) optimization-based tech-

niques were also used for control of WECs. Further details on different control strategies for WECs can be found in (Ringwood, Bacelli, & Fusco 2014).

The remainder of the paper is organized as follows. In Section 2 we introduce the model of the WEC that is later used in the case studies, which includes an array of point absorber devices, termed the floater blanket, and the single piston pump model. Subsequently, in Section 3 the model parameters and additional consideration for the case studies are presented. In Subsection 3.1, case study I is presented where the aim is to analyze the energy absorption of the floater blanket. Furthermore, in Subsection 3.2 case study II is addressed, consisting of a model predictive control strategy maximizing the energy extraction from a single point absorber that characterizes the aggregated behavior of the WEC. Lastly, conclusions are given in Section 4.

2 WAVE ENERGY CONVERTER

The WEC that we address in this paper consists of a finite one-dimensional array of point absorber devices without mechanical coupling; a sketch of such an array of floaters is shown in Figure 1, being termed the floater blanket. The motivation behind such a construction is that the second element of the floater blanket will extract energy from a smaller wave, the third one from an even smaller one, and so on as the wave energy is gradually absorbed by the device. The number of elements in the floater blanket should be determined by the desired proportion of energy capture and the overall economic feasibility of the WEC.

Each one degree-of-freedom floater in the array extracts the potential energy of ocean waves through an adaptable piston-type hydraulic pump. One of the strengths of such an ensemble is that it has the capability to harvest energy from a wide range of ocean waves. In other words, such a device will provide a type of adaptable load control.

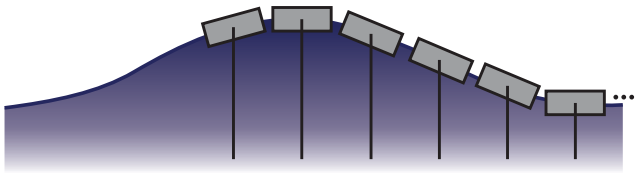

Figure 1: Floater blanket concept.

Each adaptable piston-type pump extracts the wave energy via the multi-piston pump (MPP) concept depicted in Figure 2a. In this paper, an equivalent MPP model based on a variable cylinder area A_c is used, which is shown in Figure 2b. Accordingly, the cylinder area can only take values from a finite set depending on the combination of pistons coupled; the values are shown in Table 1.

In Section 2.1, we describe the single piston pump model, which we later use in Section 3 as the effective MPP by varying the cylinder area A_c.

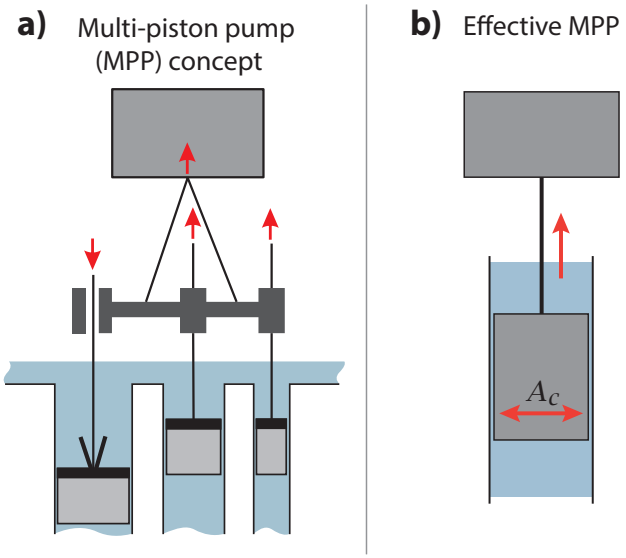

Figure 2: a) Multi-piston pump (MPP) concept consisting of three engageable pistons; b) Equivalent MPP model.

Table 1: Cylinder areas obtained through various piston combinations (0 = inactive and 1 = active).

Piston Combination {piston 1, piston 2, piston 3}	Cylinder Area A_c [m^2]
$\{1,0,0\}$	0.0149
$\{0,1,0\}$	0.0296
$\{0,0,1\}$	0.0588
$\{1,1,0\}$	0.0445
$\{1,0,1\}$	0.0738
$\{0,1,1\}$	0.0884
$\{1,1,1\}$	0.1034

2.1 *Single Piston Pump*

In this section, the model of the single piston pump (SPP) is described, which will be used for the case studies in Sections 3.1 and 3.2. A sketch of the single piston pump model is depicted in Figure 3.

Let an incident wave with height H_w, length λ_w and period T_w have a sinusoidal character with zero-mean displacement z_w (Falnes 2002) described as

$$z_w = \frac{H_w}{2} \sin\left(\frac{2\pi}{T_w} t\right). \tag{1}$$

Following the buoy displacement z_b, a cylindrical piston of height H_p, radius R_p and mass m_p moves within a cylinder of length L_c and cross-sectional area A_c to pump the working internal fluid of density ρ_{if} from a lower to an upper reservoir. The flow occupying the cross-sectional area of the cylinder A_c is channeled from a lower reservoir with cross-sectional area A_L to an upper reservoir with cross-sectional area A_U. The hydraulic heads in both reservoirs are denoted as L_L and L_U, respectively.

Considering the aforementioned buoy displacement z_b, the buoyancy force for a buoy with mass m_b, height H_b and cross-sectional area A_b is described by

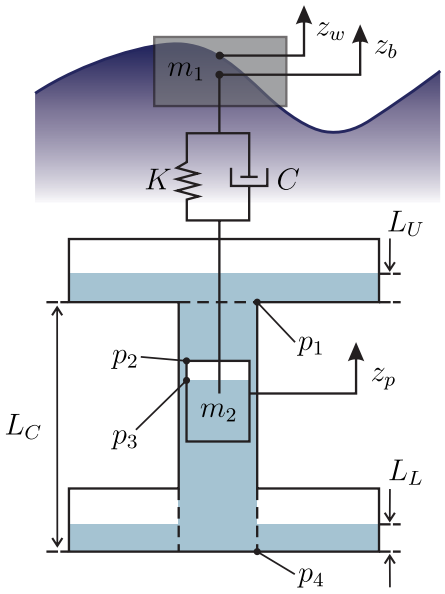

Figure 3: Single piston pump model.

the following piece-wise function of z_b and z_w as

$$F_b(z_b, z_w) = \begin{cases} 0 & \text{if} \quad D_b \leq 0, \\ \rho_{sw} g A_b D_b & \text{if} \quad 0 < D_b \leq H_b, \\ \rho_{sw} g A_b H_b & \text{if} \quad D_b > H_b, \end{cases} \tag{2}$$

where $D_b(z_b, z_w) := z_w - z_b + {}^1\!/_2 H_b$ is the amount that the buoy will be submerged, g is the gravitational acceleration constant and ρ_{sw} is the sea water density.

The equivalent mass of two ensembles are considered in the sequel, that is, the equivalent mass of the buoy and the equivalent mass of the piston-rod ensemble. There is an added mass effect when the buoy moves in a stationary fluid, being described by means of the added mass coefficient C_a (Det Norske Veritas 2011), such that

$$m_a := \begin{cases} 0 & \text{if} \quad D_b \leq 0, \\ C_a \rho_{sw} A_b D_b & \text{if} \quad 0 < D_b \leq H_b, \\ C_a \rho_{sw} A_b H_b & \text{if} \quad D_b > H_b. \end{cases} \tag{3}$$

Furthermore, we define the equivalent masses $m_1 := m_a + m_b$ corresponding to the buoy with added mass, and

$$m_2(A_c) := \begin{cases} m_{pr} + \rho_{if} L_c A_c & \text{in the upstroke,} \\ m_{pr} & \text{in the downstroke,} \end{cases} \tag{4}$$

corresponding to the mass of the piston-rod with the added water in the upstroke, where m_{pr} represents the combined mass of the piston-rod ensemble, and the internal fluid mass with density ρ_{if} is added during the upstroke mode with A_c and L_c being the cylinder's area and length, respectively.

Additionally, the buoy experiences drag and excitation forces, i.e.,

$$F_d(z_b) = -\frac{1}{2} \rho_{sw} A_b C_d \, |\dot{z}_b| \, \dot{z}_b, \tag{5}$$

and

$$F_e(z_w) = (m_a \ddot{z}_w + B \dot{z}_w + \rho_{sw} g A_b z_w) e^{-2\pi D_b / \lambda_w}, \tag{6}$$

respectively, where C_d is the drag coefficient and B is the wave damping coefficient. Furthermore, viscous friction force based on the assumption of Couette flow is considered as

$$F_f(z_p) = 2\pi R_p H_p \eta \frac{\dot{z}_p}{s_p}. \tag{7}$$

with s_p being the piston-cylinder separation, R_p being the piston radius, H_p being the piston height, and η being the viscosity of water at 20°C. This is a simplification employed for the purposes of the current work; more elaborate friction and lubrication models of the piston-cylinder interface are discussed in (Vakis & Anagnostopoulos 2016).

2.2 *Equations of Motion*

The equation of motion of the buoy can be described through Newton's second law as

$$m_1 \ddot{z}_b + B \dot{z}_b + C(\dot{z}_b - \dot{z}_p) + \rho_{sw} g A_b z_b + K(z_b - z_p) = -m_b g + F_b + F_e + F_d, \tag{8}$$

where B is the wave damping coefficient, C is the cable damping coefficient, K is the cable stiffness coefficient, F_b is the buoyancy force in (2), F_e is the excitation force in (6) and F_d corresponds to the drag force in (5). Note that (8) corresponds to a simplified Cummins' equation (Cummins 1962), where we use ordinary differential equations instead of convolution kernels to describe the radiation and excitation forces.

Analogously, the motion equation for the piston is described by the following differential equation

$$m_2 \ddot{z}_p + C(\dot{z}_p - \dot{z}_b) + K(z_p - z_b) = -m_2 g + A_c p_4 - \rho_{if} A_c \dot{z}_p^2 - F_f \tag{9}$$

where p_4 is the pressure in the lower reservoir and F_f is the viscous friction force in (7). The pressures in the upper and lower reservoir —p_1 and p_4— are related to the piston velocity by

$$\dot{p}_1 = \rho_{if} g \frac{A_c}{A_U} \dot{z}_p, \quad \text{and} \quad \dot{p}_4 = -\rho_{if} g \frac{A_c}{A_L} \dot{z}_p. \tag{10}$$

2.3 *State-space model*

In the present we make use of a nonlinear switched model that describes the operation of the WEC in the downstroke and the upstroke modes, by rewriting (8), (9) and (10) in state space form as

$$\dot{q} = Aq + f, \quad q(0) = q_0, \tag{11}$$

where the state vector is given by $q = [z_b \;\; \dot{z}_b \;\; z_p \;\; \dot{z}_p \;\; p_1 \;\; p_4]^\top$ with z_b and $\dot{z}_b$ being the position and velocity of the buoy's center of mass, respectively; z_p and $\dot{z}_p$ being the position and velocity of the piston's center of mass; lastly, p_1 and p_4 represent the pressures of the upper and lower reservoir, respectively.

Accordingly, the state matrix is given by

$$A = \begin{bmatrix} 0 & 1 & 0 & 0 & 0 & 0 \\ \frac{-\rho_{sw} g A_b - K}{m_1} & \frac{-B-C}{m_1} & \frac{K}{m_1} & \frac{C}{m_1} & 0 & 0 \\ 0 & 0 & 0 & 1 & 0 & 0 \\ \frac{K}{m_2} & \frac{C}{m_2} & \frac{-K}{m_2} & \frac{-C}{m_2} & 0 & \frac{A_c}{m_2} \\ 0 & 0 & 0 & \frac{\rho_{if} g A_c}{A_U} & 0 & 0 \\ 0 & 0 & 0 & \frac{-\rho_{if} g A_c}{A_U} & 0 & 0 \end{bmatrix} \tag{12}$$

and the affine term f in (11) becomes

$$f = \begin{bmatrix} 0 \\ \frac{-g m_b}{m_1} + \frac{F_b(x_b, x_w) + F_d(z_b) + F_e(z_w)}{m_1} \\ 0 \\ \frac{F_f(z_p)}{m_2} - g - \frac{\rho_{if} A_c \dot{z}_p^2}{m_2} \\ 0 \\ 0 \end{bmatrix}. \tag{13}$$

3 ENERGY CAPTURE OPTIMIZATION

As previously mentioned, our main results in this section focus on two aspects, namely, (I) the analysis of the wave energy extraction through a simple floater blanket system, and (II) the controller design of the adaptable piston pumps for optimal energy extraction for arbitrary wave profiles. For controller synthesis, we consider the cylinder area A_c as the control or decision variable.

Moreover, the parameters taken for the introduced model in Sections 2.1-2.3 are described in Table 2.

For the input wave, in the first case we consider a wave as in (1) with fixed height and period, which is propagated with a time shift to each element of the floater blanket; the aim here is to analyze the floater blanket energy absorption. In the second case, we consider the aggregated behavior of the whole WEC as a single point absorber, where we would like to have an adaptive system that can adjust to the wave variations; in this case, a wave profile with varying height. This will be detailed in Subsection 3.2 below.

3.1 *ENERGY MAXIMIZATION FOR THE FLOATER BLANKET*

For this first case, a simplified floater blanket without mechanical coupling is considered, consisting of an array of buoys connected to pumps as the one described by (11) without control. Building up on the previous assumptions, it is expected that certain number of buoys would be necessary to extract most of the energy available in the wave. We remark here that the heaving motion of the buoys would only extract the vertical component of the wave surge energy.

Table 2: SPP model parameters.

Parameter	Value	Description [units]
g	9.81	Gravitational acceleration [m/s^2]
ρ_{sw}	1030	Sea water density at 20°C [kg/m^3]
ρ_{if}	998.2	Water density at 20°C [kg/m^3]
η	1.002×10^{-3}	Water viscosity at 20°C [Pa· s]
K	6.87×10^{5}	Cable stiffness [N/m]
C	111.22	Cable damping [N· s/m]
H_p	0.05	Height of the piston [m]
s_p	0.001	Piston-cylinder separation [m]
R_p	0.2	Radius of the piston [m]
m_{pr}	150	Mass of piston and rod [kg]
L_c	1.83	Length of the cylinder [m]
$p_{1,0}$	3780	Initial pressure upper res. [Pa]
$p_{4,0}$	6440	Initial pressure lower res. [Pa]
m_b	1500	Buoy mass [kg]
H_b	2	Buoy height [m]
L_b	7	Buoy width [m]
A_b	49	Buoy cross-sectional area [m^2]
d_b	1	Distance between buoys [m]
C_a	1.2	Added mass coefficient [-]
C_d	1.25	Drag coefficient [-]
R_r	0.04	Radius of the rod [m]
L_r	140	Rod length [m]
A_U	49	Upper reservoir area [m^2]
A_L	49	Lower reservoir area [m^2]
$L_{U,0}$	10	Upper reservoir initial head [m]
$L_{L,0}$	30	Lower reservoir initial head [m]

We simulate a floater blanket comprised of 5 buoys, each connected to a SPP as in (11) for 50 seconds. We consider the parameters in Table 2 with $H_w = 4$m, $T_w = 10$s, and $F_f = 0$N. The assumed wave displacements, and resulting buoy displacements and buoy velocities are shown in Figure 4. Additionally, the buoy potential power and the extracted power are shown in Figure 5.

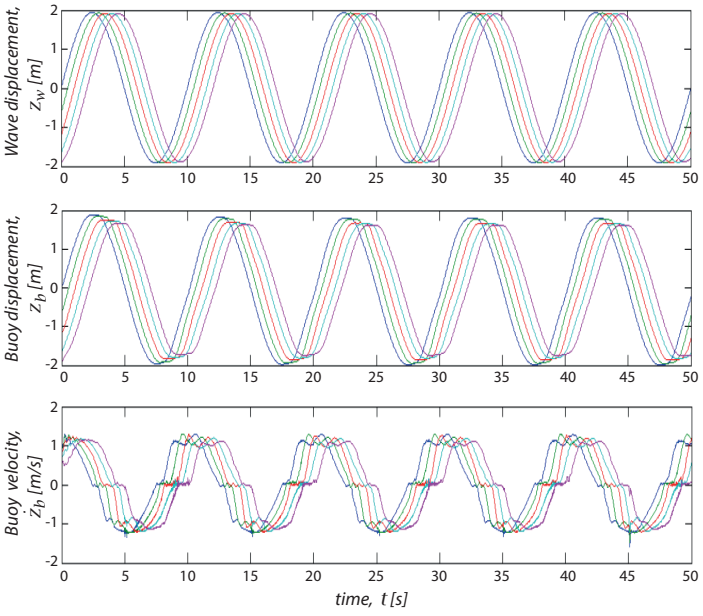

Figure 4: Wave displacement, and Buoys displacements and velocities for case study I (buoy 1 in blue, buoy 2 in green, buoy 3 in red, buoy 4 in teal and buoy 5 in purple).

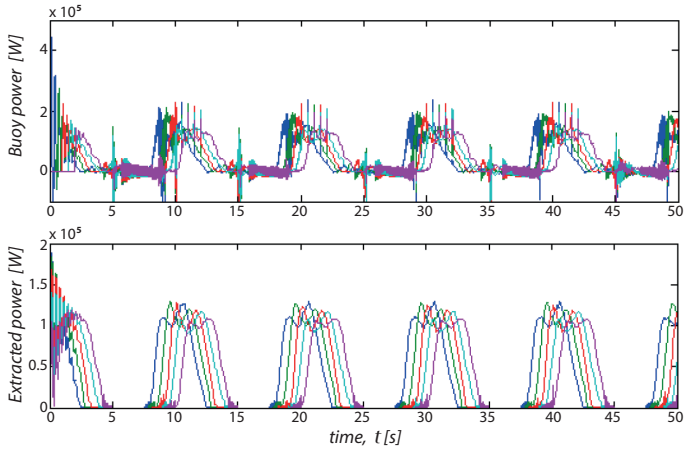

Figure 5: Buoy power and extracted power for case study I (buoy 1 in blue, buoy 2 in green, buoy 3 in red, buoy 4 in teal and buoy 5 in purple).

In Figure 5, it can be observed that the extracted power is different for every buoy, and also that the power is positive only during the upstroke and zero during the downstroke, as the pump is only pumping water during the former. At first sight, the extracted power of all pumps may seem quite similar, but after a more detailed inspection, one can see that the first pump extracts more energy, which is corroborated when the buoy and potential energy per cycle are calculated; these results are reported in Table 3. The previous is also evidenced by the decreased buoy displacement for the buoys further in the chain as depicted in Figure 4.

Table 3: Buoy energy and potential energy per cycle.

Floater Nr.	Buoy Energy [kJ]	Extracted Energy [kJ]
1	415	368
2	412	362
3	393	343
4	386	338
5	378	328
Total	1,984	1,739

Furthermore, one could try to calculate the extracted energy with respect to piston actuation following Table 1. As expected, this yields that the amount of energy extracted is directly proportional to the piston area A_c. In Section 3.2, we propose a control strategy for a single point absorber in order to obtain a better tracking of a wave profile with varying heights.

3.2 *MODEL PREDICTIVE CONTROL STRATEGY FOR A SINGLE POINT ABSORBER*

Model predictive control —often referred to just as MPC— is an optimization-based control strategy that possesses the capability of handling both complex systems and constraints. The rationale behind model predictive control is to make predictions based on the system dynamics, which are later used to solve a constrained optimal control problem formulation. Solving this problem results in an optimal sequence of controls or decisions; from this sequence, only the first one is applied and then the problem is solved once again for every subsequent step. Due to this particular way of implementing the control law, such strategies have gained the name of receding horizon strategies (Maciejowski 2002, Camacho & Bordons 2013).

3.2.1 *Optimization problem*

For the second case study, as mentioned earlier, the control variable of interest is the cylinder area, i.e., $u := A_c$, which is embedded in the model described in (11). Accordingly, we address the optimization of such an energy capture device by means of a nonlinear switched model that characterizes the aggregated behavior of the whole WEC.

We define the following cost functional for the MPC strategy, such that the buoy can follow the wave profile smoothly (i.e., without inducing high-frequency vibrations),

$$J(q,u) := Q\int_0^{T_wN} |z_b(\tau) - z_w(\tau)|\,\mathrm{d}\tau - R\int_0^{T_wN} u(\tau)\dot{z}_p^+(\tau)\,\mathrm{d}\tau \tag{14}$$

for $Q, R > 0$, where $\dot{z}_p^+ := \max\{0, \dot{z}_p\}$ is the positive component of the piston velocity, T_w is the wave period and N is the horizon —the number of incoming waves from crest to crest. The first term in (14) penalizes the distance between the buoy displacement and the wave displacement, whereas the second term aims to maximize the pumped internal fluid volume.

Hence, using the defined cost functional in (14) and the model in (11), the optimization problem corresponding to the model predictive control strategy is given by

$$\min_{u\in\mathcal{U}} \; J(q,u) \tag{15}$$

$$\text{s.t.} \begin{cases} q(0) = q_0, \\ \dot{q} = A(u)q + f(u), \\ q_{lb} \le \chi q \le q_{ub}. \end{cases}$$

over the admissible set of inputs $\mathcal{U}$, and where χ is a state selector matrix that chooses state variables which have constraints, and q_{lb} and q_{ub} are the lower-bound and upper-bound imposed on the selected state vector, respectively.

3.2.2 *Simulation Results*

In this case study, we use the SPP parameters shown in Table 2, we let the state selector matrix be $\chi = [I_4 \;\; 0_{4\times 2}]$, the lower-bounds be $q_{lb} = [130\text{m} \;\; -10\text{m/s} \;\; -10\text{m} \;\; -7\text{m/s}]^\top$, the upper-bounds be $q_{ub} = [150\text{m} \;\; 10\text{m/s} \;\; 10\text{m} \;\; 7\text{m/s}]^\top$, and

additionally we set $B = 0$Ns/m, $F_d = 0$N, $F_e = 0$N, and $F_f = 0$N. Furthermore, we consider a prediction horizon $N = 3$ —unlike standard MPC, we consider the horizon as the number of waves from crest to crest, which in this case corresponds to 3 waves. We set $Q = 20$, $R = 1$ and we first consider a wave profile with varying height as shown in Figure 6 with a total duration of $T = 60$s and height values of 6, 2, 12, 8, 4 and 10 meters, consecutively. Since we assume incoming waves with a fixed period T_w and varying height, for example as in Figure 6, we denote the discrete time step k as the sampled-time of the wave with sampling time T_w.

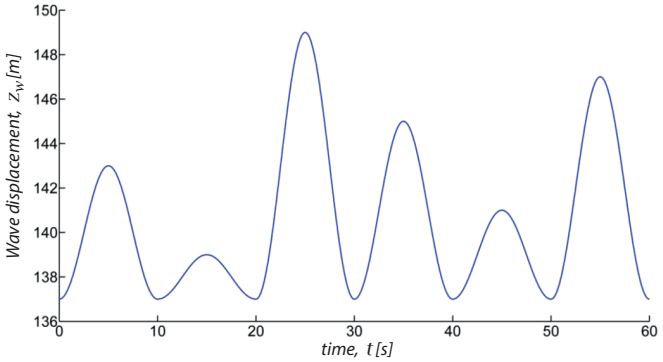

Figure 6: Input wave example for the WEC control strategy in case study II.

We remark that due to the inherent switching present in the plant model in (11) and the nature of the forces acting on the floater, such as (2), the optimization problem in (15) is of a non-convex character. However, since $\mathcal{U}$ contains only finite combinations, as presented in Table 1, we perform an exhaustive search to find the minimizer. Accordingly, for every time step k the control input is implemented in receding horizon fashion. The top part of Figure 7 shows how the buoy displacement tracks the wave displacement; moreover, in the lower part of Figure 7, the working principle of the MPC is shown, where k is the current sample instant, the implemented control input $u(k)$ is shown in green and the rest of the optimal input sequence $\{u(k+1), u(k+2)\}$ is depicted by dashed magenta lines.

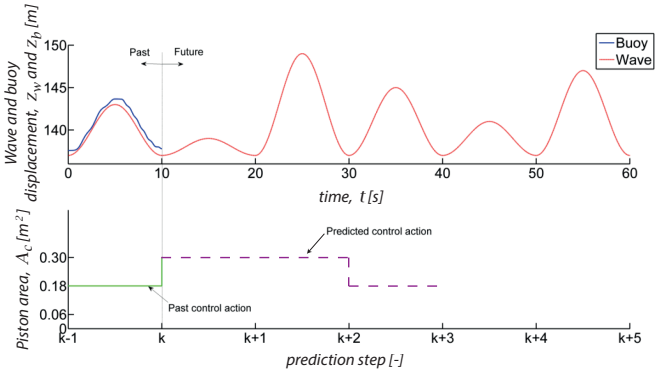

Figure 7: MPC results for a single wave sequence.

3.2.3 *Results Validation*

In order to validate the results obtained by the MPC controller, we ran the closed-loop simulation for 50 randomized cases with different wave heights instead of the one depicted in Figure 6. Furthermore, assuming a turbine efficiency of $\eta_t = 0.9$ (Drtina & Sallaberger 1999) and an electric generator efficiency of $\eta_g = 0.95$, the extracted electric energy over a simulation time T is then given by

$$E_{el} = \eta_t \eta_g \rho_{if} g L_c \int_0^T u(\tau) \dot{z}_p^+(\tau)\, \mathrm{d}\tau. \tag{16}$$

In Figure 8, a comparison of the cost in (14) and the energy extracted in (16) are shown for three cases: the case with no controller, the MPC strategy and the optimal one —namely, with infinite horizon prediction. The fact that the MPC achieves the optimal results most of the time can be seen in these plots. It is also worth noting the loss in the energy extracted when not using the MPC controller, which could have a substantial long-term impact. Moreover, there is a significant difference in the pumped water volume, which is higher using the MPC controller since it was included in the cost functional in (14). The loss of energy extracted (compared with the optimal solution) by applying the MPC algorithm is most of the times equal to zero, which means that the MPC algorithm with horizon $N = 3$ achieves the optimal solution in almost all cases.

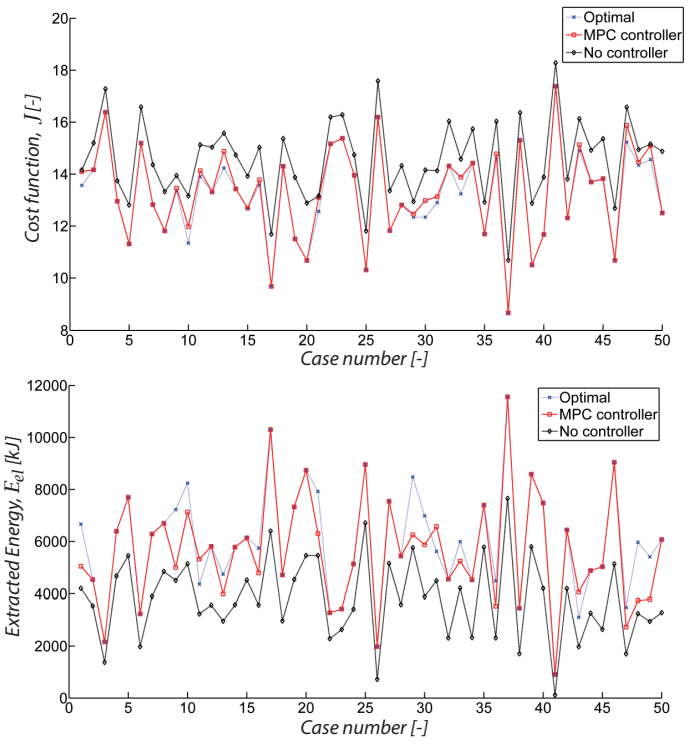

Figure 8: Cost function and extracted energy comparison for case study II for 50 randomized waves sequences.

4 CONCLUSIONS

In this paper we addressed the optimization of a specific WEC with a novel PTO system which is part of the Ocean Grazer, by means of a nonlinear switched model that describes the operation of the floaters in the down-stroke and the up-stroke modes of the WEC. Furthermore, we have investigated two case studies, the first one corresponding to the analysis of the energy extraction of a simplified floater blanket with no mechanical coupling, and the second one aiming to optimize the energy extraction of the effective MPP through a model predictive control strategy. Future work involves the design and synthesis of an MPC strategy for the whole floater blanket, the propagation of the input wave through the floater blanket, the analysis of the possible mechanical couplings between the different buoys, and the study of the storage capabilities of the WEC.

REFERENCES

Bertsekas, D. P. (1999). *Nonlinear programming*. Athena scientific.

Camacho, E. F. & C. Bordons (2013). *Model predictive control*. Springer Science & Business Media.

Cummins, W. (1962). The impulse response function and ship motions. Technical report, DTIC Document.

Det Norske Veritas (2011). Modelling and analysis of marine operations. *Offshore Standard*.

Drew, B., A. Plummer, & M. N. Sahinkaya (2009). A review of wave energy converter technology. *Proceedings of the Institution of Mechanical Engineers, Part A: Journal of Power and Energy 223*(8), 887–902.

Drtina, P. & M. Sallaberger (1999). Hydraulic turbinesbasic principles and state-of-the-art computational fluid dynamics applications. *Proceedings of the Institution of Mechanical Engineers, Part C: Journal of Mechanical Engineering Science 213*(1), 85–102.

Falnes, J. (2002). *Ocean waves and oscillating systems: linear interactions including wave-energy extraction*. Cambridge university press.

Feng, Z. & E. C. Kerrigan (2013). Latching control of wave energy converters using derivative-free optimization. In *Decision and Control (CDC), 2013 IEEE 52nd Annual Conference on*, pp. 7474–7479. IEEE.

Koca, K., A. Kortenhaus, H. Oumeraci, B. Zanuttigh, E. Angelelli, M. Cantu, R. Suffredini, & G. Franceschi (2013). Recent advances in the development of wave energy converters. In *9th European Wave and Tidal Energy Conference (EWTEC)*.

Li, G., G. Weiss, M. Mueller, S. Townley, & M. R. Belmont (2012). Wave energy converter control by wave prediction and dynamic programming. *Renewable Energy 48*, 392–403.

Maciejowski, J. M. (2002). *Predictive control: with constraints*. Pearson education.

Papalambros, P. Y. & D. J. Wilde (2000). *Principles of optimal design: modeling and computation*. Cambridge university press.

Ringwood, J. V., G. Bacelli, & F. Fusco (2014). Energy-maximizing control of wave-energy converters: The development of control system technology to optimize their operation. *Control Systems, IEEE 34*(5), 30–55.

SI-Ocean (2012). Ocean energy: state of the art. *Online report, December*.

Vakis, A. I. & J. S. Anagnostopoulos (2016). Mechanical design and modeling of a single-piston pump for the novel power take-off system of a wave energy converter. *Renewable Energy 96*, 531–547.

Vakis, A. I., H. Meijer, & W. A. Prins (2014). First steps in the design and construction of the ocean grazer. In *ASME 2014 12th Biennial Conference on Engineering Systems Design and Analysis*, pp. V002T09A004–V002T09A004. American Society of Mechanical Engineers.

van Rooij, M., H. Meijer, W. Prins, & A. Vakis (2015). Experimental performance evaluation and validation of dynamical contact models of the ocean grazer. In *OCEANS 2015-Genova*, pp. 1–6. IEEE.